Int. J. Heat Mass Transfer. Vol. 25, No. 9, pp. 1383–1395, 1982
Printed in Great Britain

0017–9310/82/091383–13 $03.00/0
Pergamon Press Ltd.

CRITICAL HEAT FLUX IN HELICAL COILS WITH A CIRCUMFERENTIAL HEAT FLUX TILT TOWARD THE OUTSIDE SURFACE

M. K. JENSEN
Department of Mechanical Engineering, The University of Wisconsin–Milwaukee, Milwaukee, WI 53201, U.S.A.

and

A. E. BERGLES
Department of Mechanical Engineering and Engineering Research Institute, Iowa State University, Ames, IA 50011, U.S.A.

(*Received* 2 *April* 1982)

Abstract—A study of the forced-convection boiling of R-113 in electrically heated coils with a substantial heat flux tilt toward the outside of the coils is reported. The circumferentially local subcooled critical heat flux (CHF) with a flux tilt is increased or decreased, when compared to a coil without a flux tilt at the same bulk fluid condition, depending on the relative magnitudes of the flux tilt, mass velocity, and ratio of tube diameter to coil diameter (d/D). Generally, there are increases in the local CHF with decreasing mass velocity and d/D, and with increasing flux tilt. The quality region CHF in a coil with a flux tilt is lower than the CHF in a coil without a flux tilt. The subcooled and quality region CHF condition (when unaffected by buoyancy) occurs at the inside surface of the coil and not at the location of highest heat flux. Operational problems, in particular upstream CHF conditions, may occur if a coiled tube is operated with low to moderate subcooling near the inlet and with moderately high heat fluxes.

NOMENCLATURE

a, radial acceleration, (V^2/D) [m s^{-2}];
Bo, boiling number, $q''/(H_{fg}G)$;
d, inside tube diameter [m];
D, coil diameter, tube axis to tube axis [m];
g, gravitational acceleration [m s^{-2}];
G, average mass velocity [kg m^{-2} s^{-1}];
Gr, Grashof number, $gd^3\,\rho_l^2\,(\rho_l - \rho_v)\,\rho_l/\mu_{sl}^2$;
H, enthalpy [J kg^{-1}];
H_{fg}, enthalpy of vaporization [J kg^{-1}];
L, heated length [m];
p, pressure [Pa];
q'', heat flux [W m^{-2}];
Re, Reynolds number, Gd/μ;
V, average axial velocity [m s^{-1}];
x, thermodynamic quality.

Greek symbols

ρ, density [kg m^{-3}];
μ, dynamic viscosity [N s m^{-2}].

Subscripts

avg, average;
c, coiled;
cr, critical;
WFT, with flux tilt;
in, inlet;
l, saturated liquid;
max, maximum;
min, minimum;
s, saturated;
str, straight;
v, saturated vapor.

INTRODUCTION

MOST coiled-tube boiling heat transfer and critical heat flux (CHF)* studies have been performed with electrically heated tubes. When the coil is being formed, the tube wall deforms so that a nonuniform heat flux distribution occurs around the circumference of the tube. The highest flux occurs at the inside surface of the tube but the nonuniformity generally is not large. In practice, however, situations can arise in which the heat flux is highest at the outside of the coil. For instance, a coiled tube is to be used as the receiver for a solar energy concentrator, the Crosbyton (Texas) System [1, 2]. For this system, the flux distribution is much more nonuniform than those previously studied and, more importantly, the maximum flux is 180° displaced from the maximum flux location in the usual electrically heated test sections. Nonuniformities in the heat flux distribution can arise also with two-fluid heat exchangers used in industry due to the bypassing of fluid flow toward the outside of the coil. The term 'flux tilt' (q''_{max}/q''_{avg}) is used to describe the heat flux nonuniformity.

Various investigators [3–12] have concluded that differences in the boiling heat transfer and pressure drop characteristics between flow in normal coils and

* The transition from highly efficient boiling or forced-convection vaporization heat transfer to inefficient vapor-dominated heat transfer occurs at the CHF condition.

in straight tubes can be attributed to the formation of a secondary flow superimposed on the main flow. A pair of generally symmetrical vortices arises due to the centrifugal force which occurs because of the coil geometry. Interpreting the results in terms of the 'local conditions hypothesis', i.e. CHF depends only on local quality for a given pressure level, mass velocity and tube diameter, the findings of these investigators are:

(1) The CHF condition in coils occurs at different bulk steam qualities at different circumferential locations, with a coiled tube, in most cases, having a higher quality at which a particular circumferential location exhibits CHF than a vertical straight tube at the same heat flux.

(2) The circumferential location of the CHF condition in coils with vertical axes appears to depend on the relative magnitudes of the centrifugal and gravitational forces.

(3) In the quality region, because of stronger centrifugal forces and secondary flows, the smaller radius coils exhibit larger critical qualities at the same heat flux.

(4) For a given coil at the same critical quality, an increase in mass velocity up to about 1000 kg m^{-2} s^{-1} usually results in an increase in the quality region CHF (which is the reverse of the situation usually found with straight tubes); further increases in mass velocity cause a decrease in CHF.

(5) In the subcooled region, the CHF at constant subcooling is lower in the coil than in a straight tube. Around zero quality a reversal occurs; over a small quality change the CHF in the coil changes from being lower to being higher than that in a straight tube.

(6) If a coiled tube is operated with low to moderate subcooling near the inlet and with moderately high heat fluxes, upstream CHF conditions may occur due to the non-monotonic shape of the CHF–x_{cr} curve.

(7) The hydrodynamics of coil flow [13, 14] show many interesting phenomena which help explain the CHF behavior.

(8) No investigations of the effect of flux tilt appear to have been previously reported for coiled tubes.

Several CHF studies for straight tubes with various flux tilts have been performed [15–24]. Important conclusions are:

(1) The CHF condition occurs at the point of the maximum heat flux (q''_{max}) around the tube perimeter.

(2) The maximum, circumferentially local CHF in subcooled and quality boiling is higher for a tube with a flux tilt than for one without a flux tilt at the same bulk enthalpy. The difference increases with increasing flux tilt.

(3) The difference in the maximum, circumferentially local CHF between tubes with and without a flux tilt decreases with increasing pressure, quality, and mass velocity.

(4) The circumferentially-averaged CHF for nonuniformly heated tubes is lower than for the uniform case at the same quality.

Dunn and Vafaie [2] studied a helical coil which was radiantly heated on one side. The focus of the study, however, was on the vaporization heat transfer coefficients prior to dryout. Very limited CHF information was presented.

The complex nature of two-phase flow in coils, further complicated by a highly nonuniform circumferential heat flux distribution, would make *a priori* CHF predictions extremely difficult using the existing straight tube or coiled tube data in the literature. Hence, this study was initiated in order to determine the effects of a nonuniform circumferential heat flux, with the highest heat flux at the outside surface, on the CHF condition in flow boiling heat transfer in helically coiled tubes. The reference tests, i.e. CHF data for straight tubes and uniformly heated coils, have been reported [12].

EXPERIMENTAL APPARATUS

A schematic of the closed flow loop is shown in Fig. 1. R-113 (dissolved gases <0.05 ppm by volume) was delivered by a variable-speed pump to the preheater/recuperator (P/R). The liquid temperature at the outlet of the P/R was controlled by adjusting the flow rate and pressure of the fluid on the shell side of the P/R. Electric preheaters downstream of the P/R were used to set the required test-section inlet temperature. A flow control valve at the test-section inlet was used to eliminate thermal-hydraulic flow instabilities. The electrically (DC) heated test sections were enclosed in a transite box. The space between the test section and walls of the box was filled with insulation so as to reduce heat loss to a negligible value. The flow was measured with rotameters. All temperatures were measured with 30 ga copper–constantan thermocouples. The thermocouple outputs as well as the voltage drop and current supplied to the test sections were automatically monitored with a Hewlett–Packard data acquisition system.

One straight, horizontal tube and three pairs of coiled tubes with vertical axes were tested (Table 1). The coils with and without a flux tilt were paired so that the effect of the nonuniform heat flux could be determined. The tube material was 316 stainless steel. After coiling, if inspection revealed ripples on the inside surface of the tube, the coil was discarded since roughness could bias the results. Some deformation in tube diameter was experienced, which resulted in a slightly oval tube, but generally the difference between the major and minor diameters was less than 0.05 mm.

To obtain the nonuniform heat flux, nickel was electrolessly plated on half of the outside diameter of the tube after the tube was coiled (Fig. 2). Since the nickel has a lower resistivity than the stainless steel base material, more of the current flowed through the nickel layer than through the stainless steel, resulting in a higher heat generation rate in that half of the tube. As a result of manufacturing problems, the 22 cm coil had a maximum nickel thickness of 0.15 mm (at the 90° location) while the other two had a maximum nickel thickness of 0.10 mm. The thickness of the nickel varied

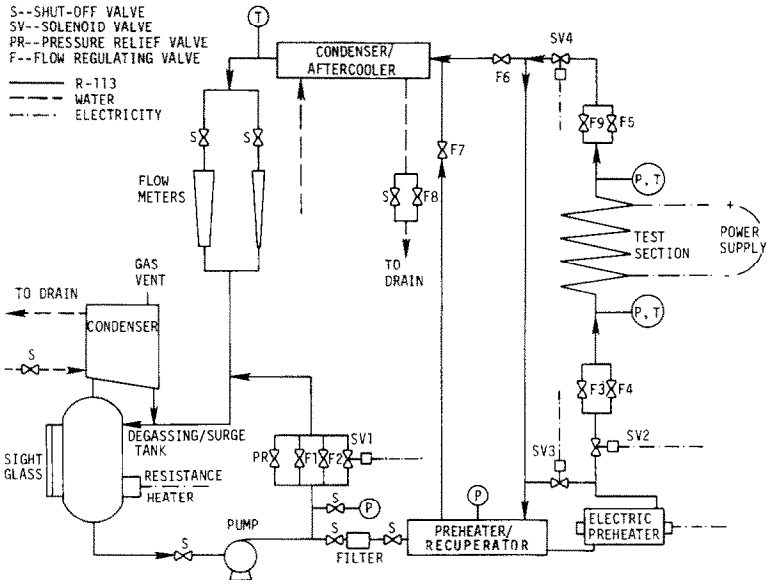

FIG. 1. Schematic layout of test loop.

0.025 mm between the 90° location and the 0° and 180° locations. This continuous variation was consistent with all three coils and was a result of the plating process. The heat flux distributions in the coiled-tube test sections are indicated in Table 2.

The wall temperatures of the coiled test sections were measured at axial and circumferential locations. The thermocouples were electrically insulated from the wall by a 0.025 mm thick layer of Teflon tape, and then securely fastened to the tube wall with additional layers of the tape. For the longer test sections, 14 axial locations were used; for the shorter test sections, 10 axial stations were used. The axial locations each had four thermocouples positioned 90° apart around the circumference.

The experimental conditions covered in this investigation were

P, 0.94 ± 0.04 MPa (at test-section outlet),
G, 570–5470 kg m^{-2} s^{-1},
q'', 54 000–940 000 W m^{-2},
x_{cr}, −0.55–+0.99,
Inlet subcooling, 0–110 K.

EXPERIMENTAL PROCEDURE

As an initial check of the experimental apparatus and procedure, single-phase heat transfer tests were performed with all coils and compared to correlations [25, 26] found in the literature. Agreement was excellent for the majority of the Reynolds number range ($7100 < Re < 120\,000$), with most of the circumferentially-averaged local heat transfer coefficients being within ±10% of the predictions. It was concluded that the nonuniform heat flux had no effect on the average heat transfer coefficients.

Testing under boiling conditions began after degassing the R-113. The test-section flow rate, pressure level, and inlet fluid temperature were set at their required levels and the test-section power was increased in small steps. After the power was increased, if one or more wall temperatures rose rapidly relative to the other wall temperatures, data were taken quickly and test-section power then was either rapidly reduced to a low level or shut-off completely.

The inside wall temperature and the heat flux were determined by solving the steady-state heat conduction equation for a circular tube. Account was taken of the plating and the circumferential variation in wall thickness, resulting from the bending process, as well as changes in heat and electrical conduction lengths and areas. The wall thickness and temperature drop were small enough that the property variation due to the temperature gradient was negligible. Circumferential conduction was found to be insignificant because of the thin tube wall, low metal thermal conductivity, and high heat transfer coefficients.

The location of the CHF condition in the straight tube was identified by noting a sharp wall temperature rise with a small increase in power. Generally, when the final power level was reached, only the last two wall thermocouples indicated a large temperature rise, with the second-to-last thermocouple not showing as steep a temperature rise as the last thermocouple. However, at lower mass velocities and heat fluxes, the elevation in temperature extended 12–15 cm along the tube. In those cases, the CHF condition (local heat flux and quality) was identified by noting the thermocouple location with approximately a 17 K rise in wall temperature. The validity of this criterion has been demonstrated [27].

The identification of the coiled tube CHF condition was basically the same as for the straight tube tests

Table 1. Test section dimensions

Test section no.	Inside tube diameter (cm)	Coil diameter (cm)	(d/D)	Heated length (cm)	Total coil length (cm)	Approx. no. of coils in heated length	Helix angle (degrees)	Pitch (cm/coil)	Tube wall thickness (mm)	Plating thickness (at 270°) (mm)
1	0.762	(straight)		63.5					0.152	
2	0.762	(straight)		127.0					0.152	
3	0.744	40.96	0.0182	129.5	762.0	1	1.78	2.540	0.254	
4	0.744	40.96	0.0182	63.5	762.0	1/2	1.78	2.540	0.254	
5	0.762	21.59	0.0353	127.0	640.1	2	1.68	1.588	0.152	
6	0.762	21.59	0.0353	125.7	501.7	2	1.68	1.270	0.152	
7	0.762	21.59	0.0353	63.5	502.9	1	1.68	1.270	0.152	
8	0.762	21.59	0.0353	63.5	393.7	1	1.68	1.270	0.152	
9	0.762	11.75	0.0649	127.0	294.6	3 1/2	3.87	1.270	0.152	
10	0.762	11.75	0.0649	63.5	296.6	1 3/4	3.87	1.588	0.152	
11	0.762	11.75	0.0649	63.5	348.0	1	3.87	1.588	0.152	
12	0.744	40.96	0.0182	129.5	624.8	1	1.78	2.540	0.254	0.102
13	0.744	40.96	0.0182	121.9	624.8	1	1.78	2.540	0.254	0.102
14	0.744	40.96	0.0182	63.5	566.4	1/2	1.78	2.540	0.254	0.102
15	0.762	21.59	0.0353	127.0	591.8	2	1.68	1.270	0.152	0.152
16	0.762	21.59	0.0353	121.9	602.0	2	1.68	1.270	0.152	0.152
17	0.762	21.59	0.0353	63.5	495.3	1	1.68	1.270	0.152	0.152
18	0.762	21.59	0.0353	63.5	408.9	1	1.68	1.270	0.152	0.152
19	0.762	21.59	0.0353	63.5	408.9	1	1.68	1.270	0.152	0.152
20	0.762	21.59	0.0353	63.5	269.2	1	1.68	1.270	0.152	0.152
21	0.762	11.75	0.0649	127.0	528.3	3 1/2	3.87	1.588	0.152	0.102
22	0.762	11.75	0.0649	127.0	401.3	3 1/2	3.87	1.588	0.152	0.102
23	0.762	11.75	0.0649	63.5	276.9	1 3/4	3.87	1.588	0.152	0.102

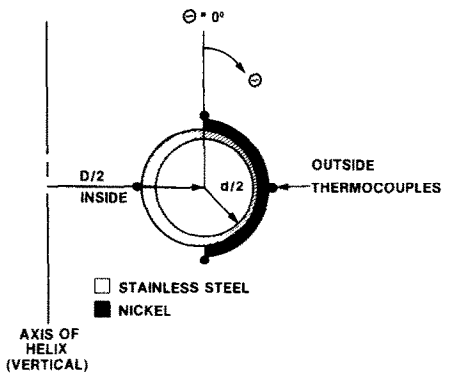

FIG. 2. Schematic (exaggerated) of geometry of WFT coil.

except that the temperature rise criterion for CHF was lowered to about 7 K. When the test-section power was raised to a value very near that required to initiate the CHF condition, one of the wall temperatures at a particular axial location would jump this amount. This temperature jump was a prelude to a large temperature excursion with a small additional increase in power. Once the CHF condition was reached at one circumferential location, the dry patch did not necessarily spread around the tube.

Inlet subcooling and test-section length both were varied to cover a range of outlet critical qualities. In the high quality region, the long tubes were used to obtain the CHF data in all cases. In the subcooled, high mass velocity region, the long tubes again were used. In the subcooled, low mass velocity region, the short tubes were used to obtain the CHF data, while in the subcooled, intermediate mass velocity region, both long and short tubes were used.

Data from 93 straight tube tests, 172 coiled-tube tests without a heat flux tilt, and 175 coiled-tube tests with a heat flux tilt were obtained, Uncertainties associated with the variables are suggested to be: q'', $\pm 2.5\%$; x, $\pm 6.6\%$; G, $\pm 2.1\%$. Further details of the experimental apparatus, procedures, and data reduction can be found in refs. [28] and [12]. Complete tabular data, are available from the first author. The reference tests will be summarized to set the stage for analysis of the flux tilt tests.

CHF IN STRAIGHT, HORIZONTAL TUBES

The CHF results for the two straight horizontal test sections are presented in Fig. 3. 'Negative quality' is used as an indication of the liquid subcooling and is defined as $(H - H_{sat})/H_{fg}$. The local conditions hypothesis seems to apply in that CHF depends only on local quality for a given pressure level and mass velocity. More scatter in the data is evident at lower mass velocities than at the higher mass velocities. Since the data shown are typical (relative to the scatter) of all the data taken, only faired-in curves will be shown on the figures for the remainder of the data.

These data exhibit the same characteristics and trends as found in previous studies performed either with water or refrigerants [29–32]. In the subcooled and low quality regions, the CHF increases with increasing mass velocity and decreases with decreasing subcooling. At low quality an inversion occurs, and the CHF then decreases with increasing quality and mass velocity. Griffel and Bonilla [31] suggest that this reversal occurs because of different mechanisms for the CHF in bubbly and annular flow. In the subcooled region, at the lowest mass velocities (G = 544 and 1046 kg m^{-2} s^{-1}), buoyancy caused severe upstream CHF conditions and erratic wall temperature profiles, and a degradation in CHF compared to vertical flow as inferred from the high mass velocity data. This behavior is consistent with that observed [29, 33–35]

Table 2. Test section heat flux distributions

d/D	Test section	Without flux tilt* $\frac{q''_{max}}{q''_{avg}}$	Without flux tilt* $\frac{q''_{max}}{q''_{min}}$	With flux tilt† $\frac{q''_{max}}{q''_{avg}}$	With flux tilt† $\frac{q''_{max}}{q''_{min}}$
0.0182	3, 4	1.049	1.099		
	12			1.237	1.396‡
	13			1.228	1.377
	14			1.238	1.398
0.0353	5–8	1.096	1.198		
	15			1.525	2.183
	16			1.531	2.203
	17			1.558	2.302
	18			1.510	2.131
	19			1.515	2.149
	20			1.522	2.171
0.0649	9–11	1.186	1.394		
	21			1.471	1.726
	22			1.382	1.531
	23			1.412	1.593

* Maximum heat flux is at inside surface.
† Maximum heat flux is at outside surface.
‡ Variations in heat flux distributions for these tubes are due to manufacturing variation.

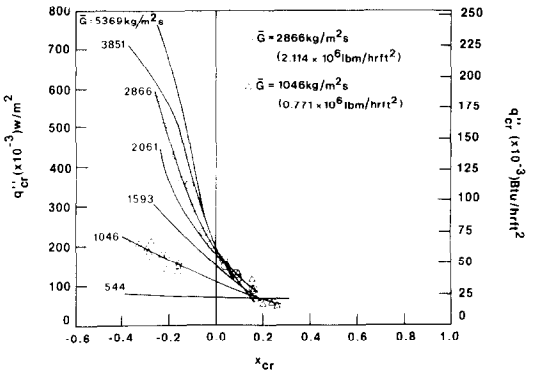

FIG. 3. Composite of straight, uniformly heated horizontal tube CHF data.

for vertical downflow and horizontal flow. These studies have shown that buoyancy reduces the CHF when compared to vertical upflow, that the main influence is in the subcooled and bubbly flow regime, and that the buoyancy effect diminishes and disappears as mass velocity increases. In this study some influence of buoyancy was observed with mass velocities as high as 2061 kg m^{-2} s^{-1}. The following correlation was developed to describe the data:

$$Bo = \frac{q''_{cr,str}}{H_{fg}G} = Re_{sl}^{-0.6}\left[1.234\text{–}3.873 \times 10^{-6} Re_{sl} + (-1.367\text{–}3.150 \times 10^{-6} Re_{sl})x\right]C \quad (1)$$

where for $Gr_{sl}/Re_{sl}^2 \geq 0.0127$

$$C = 0.4\,(Gr_{sl}/Re\ 2_{sl})^{-0.21} \quad (2)$$

and for $Gr_{sl}/Re_{sl}^2 < 0.0127$,

$$C = 1.0.$$

Taking into account the parametric distortion, thus ensuring that the heat balance equation is not violated [27], the average absolute percent deviation (AAPD) of the prediction from the experimental data is 3.9%. The data of Coffield *et al.* [30] have a value for AAPD of 10.5%.

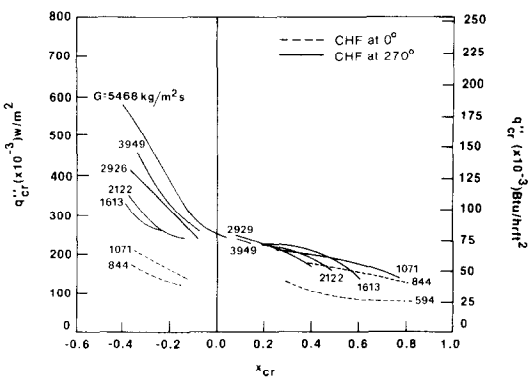

FIG. 4. Composite of local CHF data for 41 cm diameter coil without flux tilt.

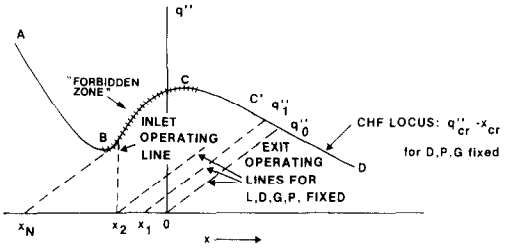

FIG. 5. Schematic representation of 'forbidden zone'.

CHF IN HELICAL COILS WITHOUT A FLUX TILT

Discussion of the CHF results

A typical plot of the coil CHF data is given in Fig. 4. An important feature of the CHF locus for each mass velocity is a region in which no data could be obtained. This 'forbidden zone' is a consequence of a minimum in the complete CHF–x_{cr} curve. This is shown schematically in Fig. 5 where the CHF–x_{cr} locus for a coiled tube is ABCD. The dashed lines are operating lines representing the quality at a particular location in the tube as the heat flux is increased. The CHF condition will occur when any of the operating lines intersects the CHF locus. For example, only an exit CHF condition would occur at $x_{in} = 0$ and $x_{in} = x_1$ (subcooled). However, if the inlet quality is reduced to x_2, the CHF condition will occur right at the tube inlet. Further reductions in x_{in} will result in additional upstream CHF conditions at the tube inlet or some downstream location until x_N is reached, after which only exit CHF's will be experienced. Points on the curve from C to C' would be unobtainable without length and/or inlet quality changes; the curve from B to C cannot be obtained without upstream CHF conditions. The complete curve was not obtained because of the impossibility of observing all the wall temperatures along the tube simultaneously and because of the difficulty of recording all of the required data in a short enough time so that the test section was not damaged or destroyed. Although similarly shaped CHF–x_{cr} curves have been presented in the literature previously (e.g. for very high mass velocities [36, 37], and for systems with upstream compressibility [38]) the probable mechanisms in the present case are different, as will be discussed below.

In the subcooled region, the CHF–x_{cr} curves decrease monotonically with decreasing subcooling. The coiled tube data are lower than the straight tube data, with the curves converging as the exit subcooling decreases. With decreasing d/D (Fig. 9) and mass velocity, the coiled tube data approach the straight tube data. At lower mass velocities, buoyancy effects were evident. For $G \leq 1000$ kg m^{-2} s^{-1}, the CHF condition generally occurred at the top of the tube while at higher mass velocities it occurred at the inner wall (Fig. 4).

The differences between the subcooled CHF condition in coiled and straight tubes appear to be

attributable to the existence of centrifugal force in the coil flow which tends to preferentially collect the vapor at the inner surface. This is aggravated by the slightly higher heat flux (Table 2) and the CHF condition occurs at a lower heat flux than in a straight tube. At lower mass velocities, and with larger coil diameters, the weaker centrifugal forces reduce the strength of the secondary flow. The reduction in CHF thus is less as coil diameter is increased. At some critical mass velocity/coil diameter combination, the buoyancy force overcomes the inertial and centrifugal forces resulting in vapor clotting at the top of the tube and little difference between straight and cooled tube CHF.

In the quality region, CHF is enhanced as a result of the radial acceleration. The data show a generally increasing CHF with increasing d/D. For a given quality, the CHF initially increases with increasing mass velocity then decreases after reaching a maximum at about $1000\,\mathrm{kg\,m^{-2}\,s^{-1}}$. As in the subcooled region, buoyancy effects were apparent between 840 and $1000\,\mathrm{kg\,m^{-2}\,s^{-1}}$ for the largest coil, and between 540 and $800\,\mathrm{kg\,m^{-2}\,s^{-1}}$ for the two smaller coils. Qualitative explanations have been proposed [12, 39, 40] to explain these trends.

The transition zone between the subcooled region with its CHF mechanism and the quality region with its much different mechanism appears to be determined approximately by the change from the bubbly flow regime to the annular flow regime. As subcooling decreases, eventually the void fraction becomes large enough to affect the flow regime. At this point, the beneficial characteristics of the quality coil flow begin to be felt. Thus, the minimum with CHF–x_{cr} curve is obtained. The curve continues upward as the quality region characteristics predominate over the detrimental subcooled CHF characteristics.

The following correlations were developed to describe the data. The subcooled CHF equation, obtained with $q''_{cr,str}$ from equation (1), is

$$\frac{q''_{cr,c}}{q''_{cr,str}} = K = 0.769(a/g)^{-0.26} \quad \text{for} \quad \frac{(a/g)}{(d/D)} > 10$$

and

$$K = 1 \qquad \text{for} \quad \frac{(a/g)}{(d/D)} \leqslant 10 \qquad (3)$$

where $a/g = V^2/(gD)$ and V is calculated assuming the total flow is liquid. The AAPD = 7.4%. The quality region equations are

for $G > 950\,\mathrm{kg\,m^{-2}\,s^{-1}}$

$$Bo = 17126\,Re_{sv}^{-1.143}\,x^{-0.436}\,(d/D)^{0.31}, \qquad (4)$$

for $G \leqslant 950\,\mathrm{kg\,m^{-2}\,s^{-1}}$

$$Bo = 0.00000409\,Re_{sv}^{0.50}\,x^{-0.460}\,(d/D)^{0.17}$$

with an AAPD = 3.0%.

CHF IN COILED TUBES WITH FLUX TILT

General characteristics of data

The operating and CHF identification procedures of the tests of the coils with a flux tilt (WFT) toward the outside surface were the same as for the normal coils. However, since the temperature rise associated with the critical condition was much faster and larger for the WFT coils than for the other coils, only the four circumferential wall temperatures at each of the last three axial stations closest to the exit were recorded. When the CHF condition occurred far upstream, the exact location was not known and no data were obtained. For certain ranges of inlet subcooling, upstream overheating (determined when the temperature at the thermocouple location 12.7 cm from the exit rose first instead of the outlet thermocouple temperature) occurred for all mass velocities for the 12 cm coil. For the other two coils, upstream overheating occurred only at the lower mass velocities ($G < 1500\,\mathrm{kg\,m^{-2}\,s^{-1}}$).

In the high quality region, the data from the normal coils and WFT coils have similar behavior, with the local CHF from the WFT coils being lower than that of the normal coils. However, in the lower quality and subcooled regions, there are significant differences in behavior between the two sets of coils. These differences depend upon mass velocity, flux tilt, and coil diameter. At high mass velocities no minima occur in the CHF–x_{cr} curves for the two large diameter WFT coils; but at lower mass velocities in the two larger WFT coils and at all mass velocities in the 12 cm WFT coil, minima do occur. Whether or not the local CHF in WFT coils is greater than, equal to, or less than the CHF in normal coils depends upon the mass velocity, flux tilt, and coil diameter.

Discussion of the CHF results

Subcooled CHF. The subcooled CHF condition in helical coils with a flux tilt toward the outside wall is a much more complex phenomenon than that in coils with uniform heat flux, and the local CHF data (local heat flux and average cross-sectional quality) for the WFT coils (Figs. 6–8) show a variety of effects when compared to the normal coil data. At lower mass velocities ($G < 1500\,\mathrm{kg\,m^{-2}\,s^{-1}}$) for the two larger WFT coils and for all of the mass velocities for the 12 cm coil, the behavior is somewhat similar to that of

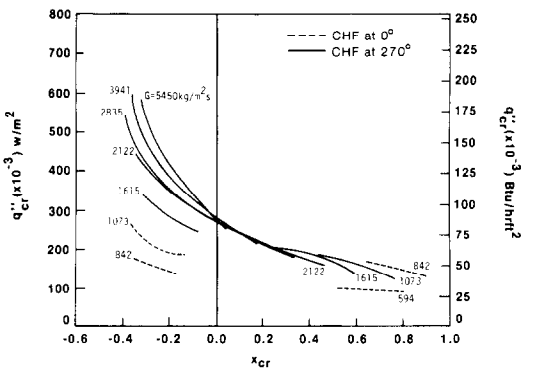

FIG. 6. Composite of local CHF data for 41 cm diameter coil with flux tilt.

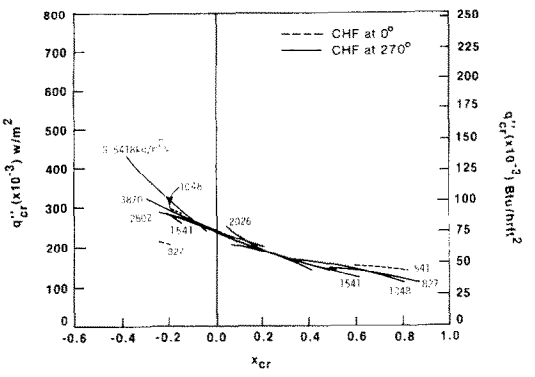

FIG. 7. Composite of local CHF data for 21.6 cm diameter coil with flux tilt.

the normal coils. At higher mass velocities, no upstream CHF conditions were encountered, and there was a smooth transition between the subcooled and quality regions to that experienced with the straight tube. Note that in both cases there is a change in slope of the CHF–x_{cr} curve at around zero quality. This suggests a change in the CHF mechanism between the subcooled and quality regions. Overall, the subcooled CHF–x_{cr} curves decrease monotonically with decreasing subcooling. As with the normal coils, the CHF's in WFT coils are lower than those of the straight tubes, with the largest degradation occurring at the largest d/D. Buoyancy effects were evident at the same mass velocities and curvature ratios as with the normal coils.

Generally, when compared to the normal coils (Fig. 9), the subcooled WFT coil data indicate a degradation in the local CHF at higher mass velocities and small coil diameter. There are improvements in the local CHF at low mass velocities. The effect of an increasing or decreasing flux tilt is somewhat obscured by the other two parameters. However, it appears as if the local CHF in the subcooled region is improved somewhat with increasing flux tilt. Qualitative explanations can be offered to explain these trends.

There is more vigorous boiling at the outer surface than at the inner because of the higher heat flux. The bubbles formed at the outside will be swept toward the

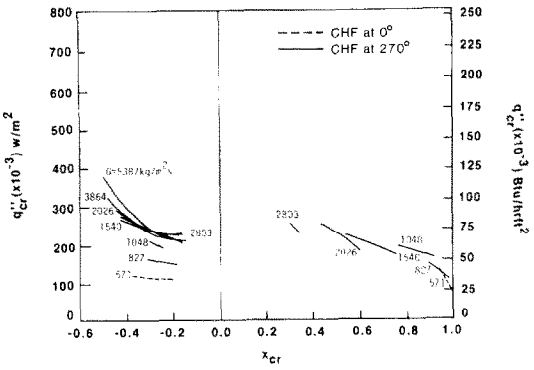

FIG. 8. Composite of local CHF data for 11.7 cm diameter coil with flux tilt.

inner surface as a result of the secondary circulation. With the heat flux decreasing as the bubbles move around the perimeter, two heat transfer processes are competing—condensation in the subcooled core and vapor generation at the wall. At a fixed flux tilt and coil diameter at lower mass velocities, the time required for the bubbles to flow around the tube perimeter is long enough so that the condensation tends to dominate and the bubbles decrease in size. With less vapor reaching the inner surface from other portions of the tube, the bubbles formed at the inner surface are the main contributors to the formation of a locally high void fraction which then would lead to the formation of a dry patch there, as in the normal coil. As the mass velocity increases, the secondary circulation increases in strength. For the bubbles in transit, there is less time for condensation, and more vapor from the outside surface reaches the inner surface. In addition, the heat fluxes are higher with the higher mass velocities and more vapor is generated than can be condensed. As a result, increasingly more degradation, when compared to the normal coiled tube, is evident with increasing mass velocity.

At the lowest mass velocity ($G \simeq 550\,\text{kg m}^{-2}\,\text{s}^{-1}$) in the two large WFT coils, no data could be obtained in the subcooled region because of upstream overheating. Examination of the upstream scorched patterns on the 22 cm and 41 cm WFT coils indicated that severe overheating occurred at the *outside* of the coil in the subcooled region but not in the 12 cm coil. There was little indication of overheating at the inside of the coil. Figure 10 can be used to explain this behavior. The solid lines are CHF–x_{cr} curves for a WFT coil. The dashed lines are the operating lines which reflect the heat flux tilt. The outside CHF conditions are not entirely obvious, as can be seen by the sketch given in Fig. 10 where the abscissa is the average cross-sectional quality. As the test section power is raised, the operating line for the outside surface intersects its CHF locus before the inside surface operating line encounters its CHF locus. It is clear that lowering of the inside CHF locus or reduction of the flux tilt can change this picture so that the CHF condition occurs at the inside rather than the outside of the tube. At this low mass velocity ($550\,\text{kg m}^{-2}\,\text{s}^{-1}$), the secondary flow is weak; thus, the flow pattern is probably not much different than that in a straight tube. In straight tubes, the CHF condition always occurs at the point of highest heat flux. Hence, at low mass velocities and large coil diameters, the WFT coil results are consistent with previous investigations with straight tubes with flux tilt.

The effect of the curvature ratio, d/D, is consistent with the above explanation for mass velocity. As d/D decreases, with a fixed flux tilt and mass velocity, there will be a weaker secondary circulation. Hence, the behavior of the heat transfer processes could be as described above for the decreasing mass velocity with fixed d/D. The local CHF will increase with decreasing d/D.

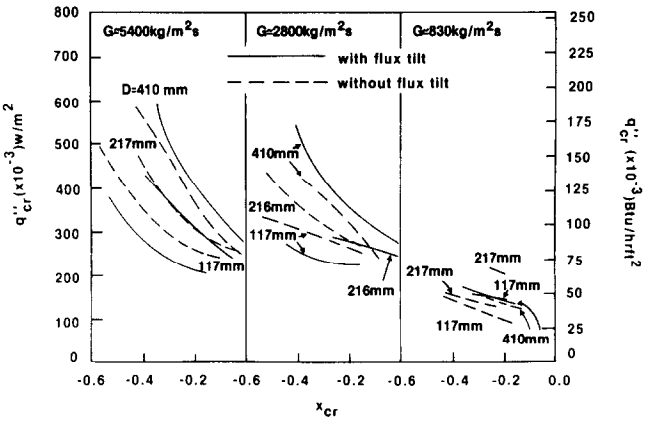

FIG. 9. Comparison of effect of mass velocity and coil diameter on local CHF in coils with and without flux tilt.

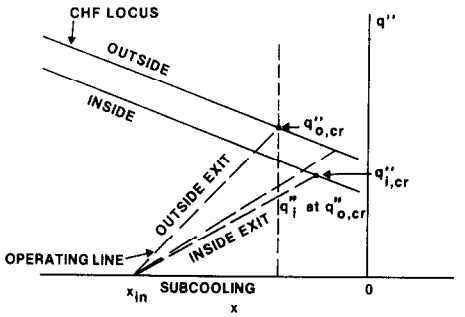

FIG. 10. Schematic (exaggerated) of CHF behavior at the inside and outside surface of a coiled tube on a local heat flux and average cross-sectional quality basis.

As mentioned above, an increasing flux tilt in the subcooled region seems to increase the local CHF. With the higher heat flux at the outside of the coil, more vigorous boiling should occur there than anywhere else on the perimeter. The secondary circulation sweeps the bubbles back toward the inner surface. But as the flux tilt increases, the relative heat flux at the inner surface decreases. The bubbles from the outside move from a 'hot' area to a 'cooler' area. The liquid here condenses the vapor much more readily than in a uniformly heated tube. In addition, the secondary flow will circulate the colder fluid away from the inner surface toward the outer surface. This could lead to a slight suppression in the growth of the vapor bubbles at the outer surface, so that the higher heat flux from the higher flux tilt might not necessarily cause larger bubbles to form at the outer surface. Consequently, the bubbles formed at the inner surface would have to be the main cause of a locally high vapor which causes the CHF condition. When compared to a normal coil, the local CHF would be higher in the coil with a flux tilt.

The preceding discussion suggests that the interactions of the mass velocity, flux tilt, and curvature ratio are quite involved. The figures showing the local data show increases, no change, and decreases in the local CHF, when compared to the normal coil, depending on the combination of these three variables. The plots of the average CHF data (Fig. 11) generally indicate an increase in the CHF, with the 22 cm WFT coil showing a substantial improvement. This could be expected since the increased heat addition is occurring at that location in the tube where the heat transfer mechanism is most efficient and where the degradation in the local CHF is not great.

Quality CHF. The effect of the higher heat flux at the outside of the coil on the local CHF in the quality region is easier to explain than its effect in the subcooled region. The shape and relative location of the local CHF curves are very similar to those of the reference coils, generally only being displaced downward (Fig. 12). The local data indicate that as q''_{max}/q''_{avg} increases, the local CHF decreases. As with the normal coiled tubes, the CHF condition at the higher mass velocities appears first at the inner surface. In straight tube investigations, the CHF condition has always been reported as occurring at the point of maximum heat flux. But even in those cases in this study where the flux tilt was 1.5, no appearance of overheating was observed on the high flux portion of the tube. The effect of buoyancy was observed at the same conditions as it was with the normal coils.

When comparing the CHF data on an average basis (Fig. 13), the CHF levels for the normal coils and WFT coils are approximately equal for the 41 cm and 22 cm coils. The data for the 12 cm WFT coil are 10–15% higher than the data from the normal coil. Whether or not the average CHF of a WFT coil is increased, appears to be a function of the flux tilt and curvature ratio.

The mechanism of the quality region CHF in coils with a flux tilt appears to be basically the same as for coils without flux tilt, but modified to account for the changes in the local conditions around the circumference of the tube. The centrifugal force caused by the fluid flow continuously deentrains liquid droplets from the vapor core; the secondary flow distributes the

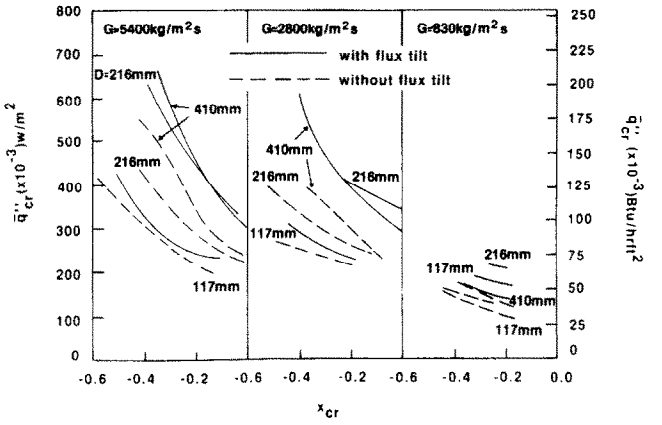

FIG. 11. Comparison of the effect of mass velocity and coil diameter on average CHF in coils with and without flux tilt.

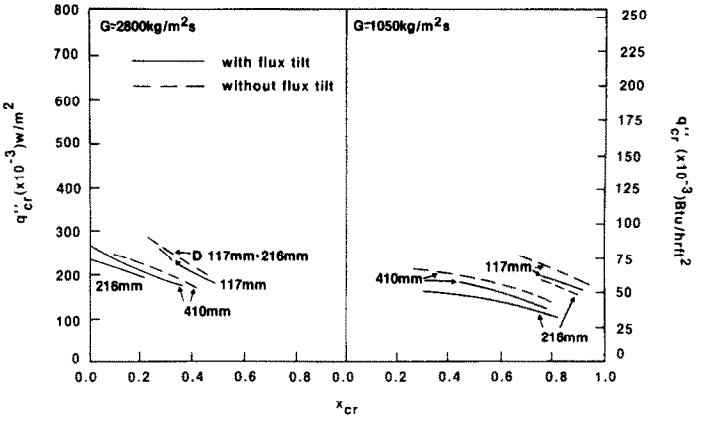

FIG. 12. Comparison of effect of mass velocity and coil diameter on local CHF in coils with and without flux tilt.

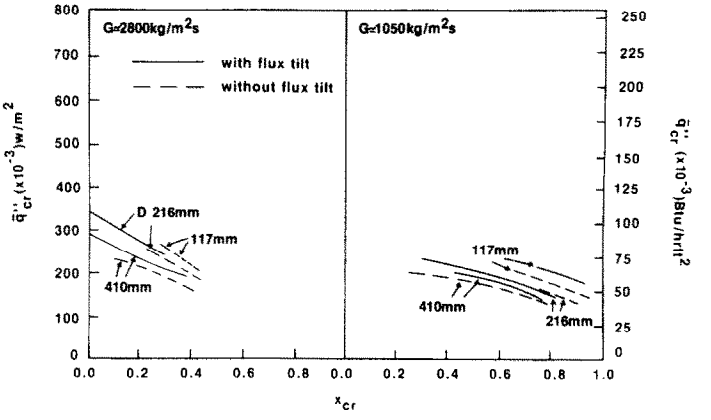

FIG. 13. Comparison of effect of mass velocity and coil diameter on average CHF in coils with and without flux tilt.

liquid over the inner surface with the liquid film flowing from the outside surface toward the inside. At the same average power, the same amount of liquid would be available in the normal coils and WFT coils. However, the nonuniform heat flux in the WFT coil disrupts or changes the film flow so that the local CHF will be lower than that in a normal coil. With the higher heat flux at the outside of the WFT coil than in a normal coil, more of the liquid film is evaporated at the outer wall. Less liquid is available to continuously flow back toward the inner wall and to keep it wet. In addition, the amount of liquid entrained from the inner surface is probably the same in both normal coils and WFT coils. As the power to the test section is raised, less and less liquid will reach the inner wall, causing the liquid film there to grow thinner. Eventually this film will break up and a dry patch will appear.

In the normal coils, the transition between the subcooled and quality regions was marked by the change in the CHF mechanism which is probably due to the change in flow regimes from a slug-type flow to annular flow. In the subcooled region in the normal tube, vapor is not distributed evenly around the circumference. The vapor tends to agglomerate at the inner surface. This behavior causes the minimum to occur in the subcooled CHF curve (e.g. Fig. 4) and causes the large differences between the normal coil and straight tube CHF–x_{cr} curves. In the WFT coils, at higher mass velocities, the vapor bubbles tend to cover more of the perimeter, with not such a large preferential agglomeration at the inner surface. The vapor distribution would approximate that in a straight tube more than that in a normal coil. Hence, the transition between the subcooled and quality regions could be expected to be more like the straight tube than the coiled tube. At the lower mass velocities, the vapor distribution again would be similar to that in a normal coil, with the resulting CHF behavior being comparable.

CORRELATION OF CHF DATA

Subcooled CHF

The three parameters influencing the subcooled CHF in WFT coils when compared to the normal coils are the mass velocity, curvature ratio, and flux tilt. Using the ratio of the CHF's from the normal coils and WFT coils, the following equation was obtained to represent the local CHF data:

$$\frac{q''_{cr,c\,WFT}}{q''_{cr,c}} = \left(0.824 + 0.222\frac{q''_{max}}{q''_{avg}}\right)(1 - 0.025\,a/g) \tag{5}$$

where $q''_{cr,c}$ is calculated from equation (3). The accleration is again calculated assuming that the total flow is liquid. The AAPD = 5.5% with the maximum deviation being 18.6%.

Quality CHF

From the examination of the data, the main parameter influencing the decrease in the local CHF is the flux tilt. The shape of the CHF–x_{cr} curves are remarkably similar so it was felt that the correlation could be in the form of a ratio between CHF's from normal coils and WFT coils. The resulting equation is

$$\frac{q''_{cr,c,WFT}}{q''_{cr,c}} = 1.291\left(\frac{q''_{max}}{q''_{avg}}\right)^{-1.551} \tag{6}$$

The normal coil CHF was calculated from equation (4). To avoid the transition effects of the lower mass velocities and of the smaller coil, only the data for $x_{cr} > 0.1$ and $G > 680\,\mathrm{kg\,m^{-2}\,s^{-1}}$ were correlated. The AAPD = 4.2% with the maximum deviation being found to be 9.9%.

CONCLUSIONS

An experimental study has been conducted to determine the effects of a nonuniform circumferential heat flux distribution, with the highest heat flux at the outside surface, on the CHF in forced-convection boiling in helically coiled tubes. The primary variables investigated were mass velocity, subcooling and quality, curvature ratio, and flux tilt. The following conclusions can be drawn from the investigation:

(1) The local, subcooled CHF in a coil with a substantial flux tilt toward the outside wall is a complex phenomenon. There can be an improvement or a degradation in the CHF, when compared to a tube without a flux tilt, depending on the relative magnitudes of the flux tilt, mass velocity, and curvature ratio. Generally, there are improvements in the local CHF with decreasing mass velocity and curvature ratio, and with increasing flux tilt.

(2) The effect of the flux tilt in the quality region is to reduce the local CHF when compared to the coil without a flux tilt. It appears that the higher flux at the outside of the coil disrupts the liquid film flowing back toward the inner surface, causing the film to be thinner than in a comparable coil without a flux tilt and thus leading to a CHF condition at a lower heat flux.

(3) The differences between the CHF's from coils with and without a flux tilt were correlated on the basis of q''_{max}/q''_{avg}. For design guidance on coils with a flux tilt, equation (5) can be used for the local CHF in the subcooled region. Equation (6) can be used for the local CHF in the quality region. The average CHF in both regions can be obtained with correlations based on data from coils without a flux tilt; however, this will tend to give conservative predictions.

More data need to be obtained, particularly at other pressures, to extend the ranges of validity of the proposed correlations and to better define the observed behavior in the subcooled and quality regions.

Acknowledgements—The investigation was supported by the Department of Mechanical Engineering and Engineering Research Institute of Iowa State University, and by the U.S. Department of Energy under contract No. EG-78-S-02-4649.

REFERENCES

1. L. D. Clements, Design considerations for the energy receiver in a fixed mirror-distributed focus (FMDF) solar energy system, Miami International Conference on Alternate Energy Sources, Miami, Florida (1977).
2. J. R. Dunn and F. N. Vafaie, Forced convection heat transfer for two-phase helical flow in a solar receiver, ASME Paper No. 81-WA/HT-13 (1981).
3. J. R. Carver, C. R. Kakarala and J. S. Slotnik, Heat transfer in coiled tubes in two-phase flow, Babcock and Wilcox Company Research Report 4438 (July 1964).
4. Z. L. Miropol'skiy and V. Y. Pikus, Critical boiling heat fluxes in curved channels, *Heat Transfer-Soviet Res.* **1**, 74–79 (1969).
5. M. Kozeki, H. Nariai, T. Furukawa and K. Kurosu, A study of helically-coiled tube once-through steam genrator, *Bull. JSME* **13**, 1485–1494 (1970).
6. V. P. Babarin, R. I. Sevasty'yanov, J. T. Alad'yev, V. F. Khuydyakov and V. A. Tkachev, Critical heat fluxes in tubular coils, *Heat Transfer-Soviet Res.* **3**, 85–90 (1971).
7. M. Cumo, G. E. Farello and G. Ferrari, The influence of curvature in post dry-out heat transfer, *Int. J. Heat Mass Transfer* **15**, 2045–2062 (1972).
8. M. Naitoh, A. Nakamura and H. Ogasawara, Dryout in helically coiled tubes of sodium heated steam generator, ASME Paper No. 74-WA/HT-48 (1974).
9. I. T. Alad'yev, V. I. Petrov, A. I. Rzayev and V. F. Khudyakov, Heat transfer in a sodium–potassium heat exchanger (Potassium boiler) made of helically coiled tubes, *Heat Transfer-Soviet Res.* **8**, 1–16 (1976).
10. F. Campolunghi, M. Cumo, G. Ferrari and G. Palazzi, Full scale tests and thermal design correlations for coiled once-through steam generators, CNEN Report No. RT/ING(75)11 (1975).
11. Z. L. Miropol'skiy, V. J. Picus and M. E. Shitsman, Regimes of deteriorated heat transfer at forced flow of fluids in curvilinear channels, *Proc. 3rd Int. Heat Transfer Conf.*, Chicago, Vol. 2, pp. 97–101 (1966).
12. M. K. Jensen and A. E. Bergles, Boiling heat transfer and critical heat flux in helical coils, *Trans. Am. Soc. Mech. Engrs*, Series C, *J. Heat Transfer* **103**, 660–666 (1981).
13. S. Banerjee, E. Rhodes and D. S. Scott, Film inversion of co-current two-phase flow in helical coils, *A.I.Ch.E. Jl* **13**, 189–191 (1967).
14. P. B. Whalley, Air–water two-phase flow in a helically coiled tube, *Int. J. Multiphase Flow* **6**, 345–356 (1980).
15. Z. L. Miropolskii and I. L. Mostinskii, Critical heat flux in uniform and non-uniform heating of the circumference of steam generating tubes, *Teploenergetika* **5**, 64–69 (1958).
16. M. A. Styrikovich and I. L. Mostinskii, The influence of non-uniform heating of the perimeter of a tube on the critical heat flow, *Soviet Physics-Doklady* **4**, 794–797 (1960).
17. I. L. Mostinskii, Influence of the conditions at the entrance on the boiling crisis in nonuniformly heated tubes, *Inzhenerno-Fizicheskii Zh.* **3**, 5–10 (1960).
18. G. V. Alekseev, B. A. Zenkevich, D. V. Remizov, D. L. Peskov, N. D. Sergeev and V. I. Subbotin, Burnout heat fluxes under forced water flow, 3rd U.N. International Conference on the Peaceful Uses of Atomic Energy, paper A/CONF 28/p/327a (May 1964).
19. G. V. Alekseev, D. L. Peskov, O. V. Remizov, N. D. Sergeev, B. A. Zenkevich and V. I. Subbotin, Critical heat flux densities with forced flow of water, *Thermal Engng* **12**, 60–64 (1965).
20. A. P. Ornatskii and L. S. Vinyarskii, Heat transfer crisis in a forced flow of underheated water in small-bore tubes, *High Temp.* **3**, 400–406 (1965).
21. D. H. Lee, Burnout in a channel with non-uniform circumferential heat flux, AEEW-R477 (March 1966).
22. D. Butterworth, A model for predicting dryout in a tube with a circumferential variation in heat flux, UKAEA Report No. AERE-M2436 (March 1971).
23. B. Chojnowski and P. W. Wilson, Critical heat flux for large diameter steam generating tubes with circumferentially variable and uniform heating, *Heat Transfer*-1974 **4**, 260–264, JSME: Tokyo (1974).
24. O. V. Remizov and A. P. Sapankevich, Burnout with non-uniform distribution of heat flux over the perimeter of a round tube, *Thermal Engng* **22**, 81–84 (1975).
25. R. A. Seban and E. F. McLaughlin, Heat transfer in tube coils with laminar and turbulent flow, *Int. J. Heat Mass Transfer* **6**, 387–395 (1963).
26. Y. Mori and W. Nakayama, Study on forced convection heat transfer in curved pipes (Second report, turbulent region), *Int. J. Heat Mass Transfer* **10**, 37–59 (1967).
27. A. W. Bennett, G. F. Hewitt, H. A. Kearsey and R. K. F. Keeys, Heat transfer to steam–water mixtures flowing in the uniformly heated tubes in which the critical heat flux has been exceeded, AERE Report No. R-5373 (1967).
28. M. K. Jensen, Boiling heat transfer and critical heat flux in helical coils, Ph.D. dissertation, Iowa State University (1980).
29. M. Merilo, Critical heat flux experiments in a vertical and horizontal tube with both Freon-12 and water as coolant, *Nucl. Engng Des.* **44**, 1–16 (1977).
30. R. D. Coffield, W. M. Rohrer Jr. and L. S. Tong, A subcooled DNB investigation of R-113 and its similarity to subcooled water DNB data, *Nucl. Engng Des.* **11**, 143–153 (1969).
31. J. Griffel and C. F. Bonilla, Forced convection boiling burnout for water in uniformly heated tubular test-sections, *Nucl. Engng Des.* **2**, 1–35 (1969).
32. Y. Katto, On the heat flux/exit-quality type correlation of CHF of forced convection boiling in uniformly heated vertical tubes, *Int. J. Heat Mass Transfer* **24**, 533–539 (1981).
33. C. Rounthwaite and M. Clouston, Heat transfer during evaporation of high quality water–steam mixtures flowing in horizontal tubes, *Proc. 2nd Int. Heat Transfer Conf.*, Boulder, pp. 200–211 (1961).
34. M. A. Styrikovich and Z. L. Miropol'skiy, *Dokl. Akad. NAUK SSSR* **71**, 2 (1950).
35. M. Merilo, Fluid-to-fluid modeling and correlation of flow boiling crisis in horizontal tubes, *Int. J. Multiphase Flow* **5**, 313–325 (1979).
36. E. D. Waters, J. K. Anderson, W. L. Thorne and J. M. Batch, Experimental observations of upstream boiling burnout, *Chem. Engng Prog. Symp. Ser.* **61** (57), 230–237 (1965).
37. D. C. Groeneveld, The occurrence of upstream dryout in uniformly heated channels, *Heat Transfer*-1974 **4**, 265–169, JSME: Tokyo (1974).
38. I. T. Aladyev, Z. L. Miropol'skiy, V. E. Doroshchuk and M. A. Styrikovich, Boiling crisis in tubes, *Proc. 2nd Int. Heat Transfer Conf.*, Boulder, pp. 237–243 (1961).
39. A. Owhadi, K. J. Bell and B. Crain, Jr., Forced convection boiling heat transfer inside helically-coiled tubes, *Int. J. Heat Mass Transfer* **11**, 1779–1793 (1968).
40. B. Crain, Jr. and K. J. Bell, Forced convection heat transfer to a two-phase mixture of water and steam in a helical coil, *A.I.Ch.E. Symp. Ser.* **69**, (131), 30–36 (1973).

FLUX CRITIQUE DE CHALEUR DANS DES SERPENTINS AVEC UN FLUX CIRCONFERENTIEL CROISSANT VERS LA SURFACE EXTERNE

Résumé—On rapporte l'étude de l'ébullition de R113 en convection forcée dans des serpentins chauffés électriquement avec une sensible croissance de flux thermique vers l'extérieur du serpentin. Le flux critique (CHF) local avec un flux variable est augmenté ou diminué, comparé au cas du flux uniforme avec la même condition de débit, selon l'amplitude relative de la décroissance du flux, la vitesse, le rapport du diamètre du tube à celui du serpentin (d/D). Généralement, il y a un accroissement du CHF local avec la décroissance de la vitesse massique et de d/D et avec l'augmentation de l'amplitude du flux. La qualité en région CHF dans un serpentin avec flux variable est plus faible qu'un flux uniforme. Des problèmes opérationnels, dans des conditions particulières en amont, peuvent apparaitre si un tube courbe est utilisé avec un sous-refroidissement faible à modéré près de l'entrée et avec des flux thermiques modérément élevés.

DIE KRITISCHE WÄRMESTROMDICHTE IN SPIRALROHRSCHLANGEN MIT EINEM WÄRMESTROMDICHTE-GRADIENTEN IN UNFANGSRICHTUNG NACH AUSSEN

Zusammenfassung—Es wird über eine Untersuchung des Siedens bei erzwungener Konvektion von R-113 in elektrisch beheizten Spiralrohren mit einem wesentilichen Wärmestromdichte-Gradienten zur Außenseite der Spiralen berichtet. Im Vergleich mit einem Spiralrohr ohne Wärmestromdichte-Gradient bei gleichen Zuständen im Strömungskern nimmt die örtrliche kritische Wärmestromdichte (CHF) in Umfangsrichtung bei unterkültem Sieden sowohl zu als auch ab—abhängig von den relativen Größen von Wärmestromdichte-Gradient, Massenstromdichte und Durchmesser-Verhältnis von Rohr und Spirale (d/D). Im allgemeinen ergibt sich eine Zunahme der örtlichen CHF-Werte bei Abnahme von Massenstromdichte und d/D und bei zunehmendem Wärmestromdichte-Gradienten.

Die kritische Wärmestromdichte bei Dampfgehalt ist in einer Spirale mit Wärmestromdichte-Gradienten kleiner als in einer Spirale ohne Gradienten. Bei unterkühltem Sieden wie auch bei Dampfgehalt tritt die CHF-Bedingung auf der Innenseite der Spirale und nicht am Ort der höchsten Wärmestromdichte auf (sofern Auftriebseffekte ohne Einfluß sind). Schwer zu beherrschende Betriebszustände—speziell stromauf gelegene CHF-Bedingungen—können auftreten, wenn eine Spiralrohrschlange mit geringer bis mäßiger Unterkühlung am Eintritt und bei mäßig holen Wärmestromdichten betrieben wird.

КРИТИЧЕСКИЙ ТЕПЛОВОЙ ПОТОК В ВИНТООБРАЗНЫХ ЗМЕЕВИКАХ С НЕОДНОРОДНЫМ ПО ПЕРИМЕТРУ РАСПРЕДЕЛЕНИЕМ ТЕПЛОВОГО ПОТОКА

Аннотация—Проведено исследование кипения с вынужденной конвекцией фреона-113 в нагреваемых электрическим током змеевиках, имеющих значительный угол наклона теплового потока по отношению к внешней поверхности. Величина локально недогретого критического теплового потока (КТП) по окружности змеевика с наклоном потока увеличивается или уменьшается (по сравнению со змеевиком без наклона потока при тех же условиях в объеме жидкости) в зависмости от наклона потока, массовой скорости и отношения диаметра трубы к диаметру змеевика (d/D). В общем случае отмечено увеличение локального критического теплового потока с уменьшением массовой скорости и отношения d/D и с увеличением угла наклона потока. Величина КТП в диапазоне весового паросодержания в змеевике с наклоном потока ниже, чем в змеевике без наклона. Возникновение КТП в диапазоне недогрева и весового паросодержания (при отсутствии влияния плавучести) наблюдается на внутренней поверхности змеевика, но не в месте подвода максимального теплового потока. Может отмечаться неустойчивый режим работы, особенно в начале возникновения КТП в тех случаях, когда во входном участке змеевика имеется большой или средний недогрев при довольно высоком подводе тепла.